

Substrate impact on the thickness dependence of vibrational and optical properties of large area MoS₂ produced by gold-assisted exfoliation

S. E. Panasci^{1,2}, E. Schilirò¹, F. Migliore³, M. Cannas³, F. M. Gelardi³, F. Roccaforte¹, F. Giannazzo^{1*} and S. Agnello^{3,1,4}.

¹ Institute for Microelectronic and Microsystems (CNR-IMM), Z.I. VIII Strada 5, 95121, Catania, Italy

² Department of Physics and Astronomy, University of Catania, Via Santa Sofia 64, 95123 Catania, Italy

³ Department of Physics and Chemistry Emilio Segre', University of Palermo, Via Archirafi 36, 90123 Palermo, Italy

⁴ ATeN Center, University of Palermo, Viale delle Scienze Ed. 18, 90128 Palermo, Italy

*E-mail: filippo.giannazzo@imm.cnr.it

Abstract

The gold-assisted exfoliation is a very effective method to produce large-area (cm²-scale) membranes of molybdenum disulfide (MoS₂) for electronics. However, the strong MoS₂/Au interaction, beneficial for the exfoliation process, has a strong impact on the vibrational and light emission properties of MoS₂. Here, we report an atomic force microscopy (AFM), micro-Raman (μ -R) and micro-Photoluminescence (μ -PL) investigation of 2H-MoS₂ with variable thickness exfoliated on Au and subsequently transferred on an Al₂O₃/Si substrate. The E_{2g} - A_{1g} vibrational modes separation $\Delta\omega$ (typically used to estimate MoS₂ thickness) exhibits an anomalous large value ($\Delta\omega \approx 21.2$ cm⁻¹) for monolayer (1L) MoS₂ on Au as compared to the typical one ($\Delta\omega \approx 18.5$ cm⁻¹) measured on 1L MoS₂ on Al₂O₃. Such substrate-related differences, explained in terms of tensile strain and p-type doping arising from the MoS₂/Au interaction, were found to gradually decrease while increasing the number of MoS₂ layers. Furthermore, μ -PL spectra for 1L MoS₂ on Au exhibit a strong quenching and an overall red-shift of the main emission peak at 1.79

This is the author's peer reviewed, accepted manuscript. However, the online version of record will be different from this version once it has been copyedited and typeset.

PLEASE CITE THIS ARTICLE AS DOI: 10.1063/1.50062106

eV, compared to the 1.84 eV peak for 1L MoS₂ on Al₂O₃. After PL spectra deconvolution, such red shift was explained in terms of a higher trion/exciton intensity ratio, probably due to the higher polarizability of the metal substrate, as well as to the smaller equilibrium distance at MoS₂/Au interface.

Keywords: MoS₂, exfoliation, gold, large area, Atomic Force Microscopy, Raman, Photoluminescence

In the last years, molybdenum disulfide (MoS₂) have been widely investigated, due to the broad range of potential applications in the fields of optoelectronics, nanoelectronics, sensing and energy [1,2,3,4]. Several synthesis methods of MoS₂ films have been explored so far, including top-down and bottom-up methods [5]. While the highest electronic quality MoS₂ is still produced by mechanical exfoliation, the micrometer size of the flakes obtained by this approach makes it unsuitable for practical applications. In this context, gold-assisted mechanical exfoliation has recently received increasing attention as an effective method to separate large area (cm²-scale) MoS₂ with excellent electronic quality from molybdenite crystals [6,7,8,9]. Since the interaction between sulfur and Au atoms [10] is stronger than the interlayer Van der Waals (VdW) bonds in the layered crystal, ultra-thin membranes (predominantly composed by monolayer (1L) MoS₂, but also containing bilayer (2L) and few-layer (FL) regions) are obtained simply pressing a bulk MoS₂ stamp on a clean Au surface. These membranes can be subsequently transferred to insulating or semiconductor substrates to fabricate electronic/optoelectronic devices, showing performances comparable to those obtained with the best quality mechanically exfoliated MoS₂ [7]. Furthermore, as-exfoliated 1L MoS₂ on Au electrodes have been employed for memristor applications [11]. Finally, the Au-assisted exfoliation has been recently extended to a large number of layered crystals beyond MoS₂, including other transition metal dichalcogenides (MoSe₂, MoTe₂, 1T-MoTe₂, WS₂, WSe₂, WTe₂, TiS₂, TiSe₂, IrTe₂, SnS₂, SnSe₂, NbSe₂, NbTe₂, VSe₂, TaS₂, TaSe₂,

This is the author's peer reviewed, accepted manuscript. However, the online version of record will be different from this version once it has been copyedited and typeset.

PLEASE CITE THIS ARTICLE AS DOI: 10.1063/1.50062106

PdSe₂), metal monochalcogenides (e.g., GaS), black-phosphorus, black-arsenic, metal trichlorides (RuCl₃), and magnetic compounds (Fe₃GeTe₂) [12]. Hence, it represents a powerful method for the realization of artificial vdW heterostructures [13,14,15] and hybrid 2D/bulk semiconductor devices [16,17,18].

The strong MoS₂/Au interaction, which is beneficial for the large-area exfoliation process, has a strong impact on the electronic, vibrational and light emission properties of MoS₂. Different studies have been reported on the strain and doping of 1L MoS₂ induced by the gold substrate [6,9]. In this context, investigating the Au substrate effects on MoS₂ vibrational and light emission properties as a function of layers number deserves a great interest. In particular, it is crucial to evaluate the changes of these properties in the two main steps of Au-assisted exfoliation, i.e. on as-exfoliated MoS₂ on Au and after transfer to the final insulating substrate.

In this paper, the evolution of Raman and photoluminescence (PL) spectra of large-area MoS₂ (firstly exfoliated on Au and subsequently transferred on an insulating Al₂O₃/Si substrate) was investigated as a function of the number of layers, evaluated by atomic force microscopy (AFM). We found that the separation $\Delta\omega$ between the in-plane (E_{2g}) and out-of-plane (A_{1g}) vibrational modes, typically used to estimate MoS₂ thickness, exhibits an anomalous large value ($\Delta\omega\sim 21.2\text{ cm}^{-1}$) for 1L MoS₂ on Au as compared to 1L MoS₂ transferred on Al₂O₃ ($\Delta\omega\sim 18.5\text{ cm}^{-1}$). Such substrate-related difference was found to gradually decrease while increasing the number of MoS₂ layers. Furthermore, PL spectra for 1L MoS₂ on Au exhibit a strong quenching and an overall red-shift of the main emission peak at 1.79 eV, compared to the 1.84 eV peak for 1L MoS₂ on Al₂O₃. Such red shift was explained in terms of a higher trion/exciton intensity ratio, probably due to the higher polarizability of the metal substrate, as well as to the smaller equilibrium distance at MoS₂/Au interface.

The Au samples employed for the exfoliation were prepared by sequential deposition of 10 nm Ni adhesion layer and 15 nm Au film on a SiO₂(900 nm)/Si substrate with DC magnetron sputtering

This is the author's peer reviewed, accepted manuscript. However, the online version of record will be different from this version once it has been copyedited and typeset.

PLEASE CITE THIS ARTICLE AS DOI: 10.1063/1.50062106

(Quorum Q300TDPLUS). A bulk MoS₂ stamp obtained by a freshly cleaved 2H-MoS₂ crystal was pressed on the Au substrate immediately after sputtering to prevent the adsorption of contaminants on the Au surface, that could reduce the exfoliation yield [6]. The 2H-MoS₂ membrane exfoliated on Au was finally transferred onto an insulating substrate, consisting of 100 nm Al₂O₃ deposited on Si. The transfer procedure consisted in the transfer of the Au/MoS₂ stack on the Al₂O₃ surface and the final etching of Au with a KI/I₂ solution [19].

The thickness of MoS₂ was evaluated by tapping mode Atomic Force Microscopy (AFM) using a DI3100 equipment by Bruker. The morphology and phase images were acquired simultaneously using sharp silicon tips with a curvature radius of 5 nm. Micro-Raman (μ -R) and micro-Photoluminescence (μ -PL) spectra were obtained using a Horiba Raman system with a confocal microscope (100 \times) and a laser excitation wavelength of 532 nm. The laser power was filtered with a neutral density (ND) filter at 1% for both spectroscopy methods. A grating of 1800 lines/mm was used to acquire Raman spectra meanwhile a grating of 600 lines/mm to acquire PL spectra. All the spectra were calibrated with respect to the Si peak at 520.7 cm⁻¹.

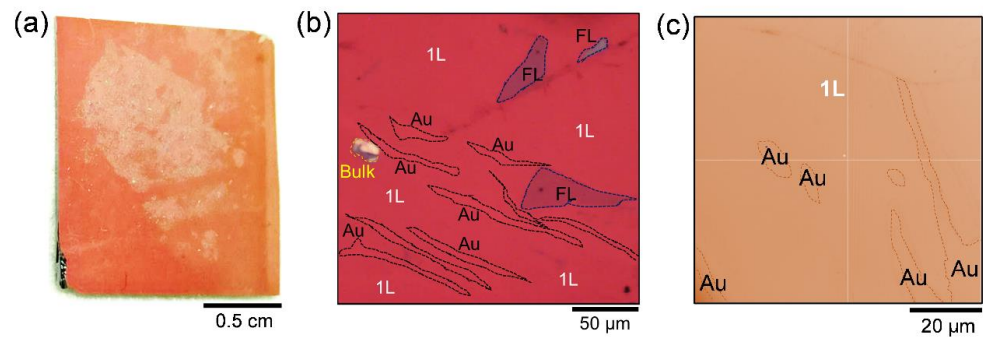


Figure 1. (a) Photograph and (b-c) optical microscopy images at two different magnifications of the large area MoS₂ membrane on the Au substrate.

This is the author's peer reviewed, accepted manuscript. However, the online version of record will be different from this version once it has been copyedited and typeset.

PLEASE CITE THIS ARTICLE AS DOI: 10.1063/1.50062106

Figure 1(a) shows a photograph of the cm^2 -scale MoS_2 exfoliated on the Au substrate, whereas two optical microscopy images at different magnifications are reported in Fig.1(b) and (c), respectively. The variable optical contrast reveals that the MoS_2 membrane is predominantly composed by 1L areas, with the presence of FL regions (violet color) and some Au uncovered areas.

After a preliminary identification of 1L and FL areas in the exfoliated MoS_2 on Au by observation of the optical contrast, the number of layers was precisely evaluated by tapping mode AFM.

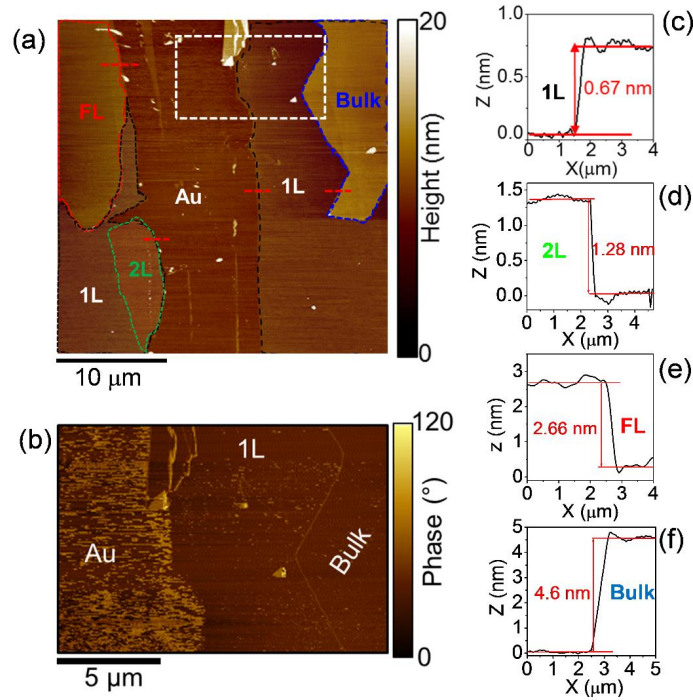


Figure 2. (a) Morphological AFM image of a region of the exfoliated MoS_2 membrane on Au, containing areas with different MoS_2 thicknesses (1L, 2L, FL and bulk) and bare Au areas. (b) Phase image corresponding to the white dashed rectangular region in (a), showing a different contrast between bare Au and MoS_2 covered regions. Height line scans from (c) 1L, (d) 2L, (e) FL and (f) bulk MoS_2 areas in panel (a).

This is the author's peer reviewed, accepted manuscript. However, the online version of record will be different from this version once it has been copyedited and typeset.

PLEASE CITE THIS ARTICLE AS DOI: 10.1063/1.50062106

Fig.2(a) shows an AFM image collected in a region comprising both a bare Au area and MoS₂ covered regions with 1L, 2L, FL and multi-layer (bulk) thickness, indicated by different color dashed lines. A phase map collected in the rectangular region indicated by the white dashed line is also reported in Fig.2(b). This image is complementary to the morphology, as it provides a clear identification of the bare Au areas with respect to the MoS₂ covered ones, thanks to the very different phase contrast. Fig.2(c) shows a representative height line-scan across the region partially covered by 1L MoS₂, from which a ~ 0.67 nm step was evaluated, consistent with the nominal monolayer thickness of 0.65 nm [1]. Furthermore, the 2L, FL and bulk thicknesses of the different areas in the morphological image are confirmed by the line-scans reported in Fig.2(d), (e) and (f), respectively. Preliminary optical contrast inspection followed by AFM analyses was also employed to identify regions with different thickness in the MoS₂ membranes transferred onto the Al₂O₃/Si substrate.

In the following, the impact of the two different substrates (Au and Al₂O₃) on the vibrational and optical emission properties of MoS₂ areas with different thickness has been investigated by μ -R and μ -PL spectroscopy. Fig.3(a) and (b) report a comparison of typical Raman spectra collected on 1L, 2L, FL and bulk regions of the MoS₂ membranes exfoliated on Au (a) and transferred onto Al₂O₃ (b). Here, the FL region corresponds to 4 layers of MoS₂, while the bulk region was formed by 10 layers of MoS₂. The characteristic in-plane (E_{2g}) and of the out-of-plane (A_{1g}) vibrational modes are observed in the spectral range from 370 to 420 cm⁻¹. All the spectra were normalized with respect to the A_{1g} peak intensity. Furthermore, vertical dashed lines, corresponding to the E_{2g} and A_{1g} peak positions for 1L MoS₂ on Au and Al₂O₃, have been reported as a guide for the eye in Fig.3(a) and (b). It can be observed how both the individual peak positions and their separation exhibit a very peculiar dependence on the kind of substrate. While a value of $\Delta\omega \approx 18.5$ cm⁻¹ is measured for 1L MoS₂ transferred onto Al₂O₃, in the case of 1L MoS₂ exfoliated on Au the E_{2g} and A_{1g} peaks exhibit a significant red and blue shift, respectively, resulting in a larger value of $\Delta\omega \approx 21.2$ cm⁻¹. Furthermore, a different behaviour of the in-plane and out of plane

This is the author's peer reviewed, accepted manuscript. However, the online version of record will be different from this version once it has been copyedited and typeset.

PLEASE CITE THIS ARTICLE AS DOI: 10.1063/1.50062106

vibrational modes is observed on the two different substrates with increasing the number of layers, as shown in Fig.3(c).

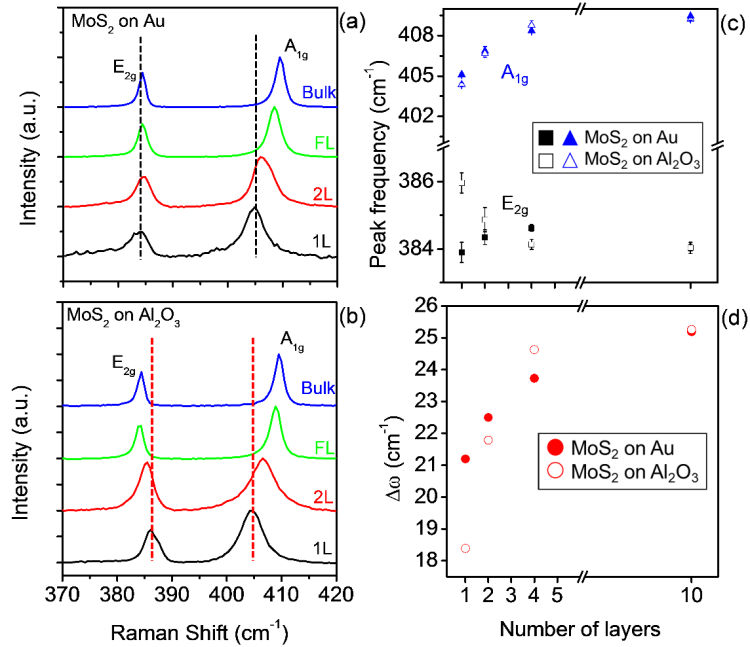


Figure 3. Typical Raman spectra of exfoliated MoS₂ on the Au substrate (a) and transferred onto Al₂O₃/Si (b) measured on 1L, 2L, FL and bulk MoS₂ regions. The black (red) dashed lines indicate the E_{2g} and A_{1g} peaks frequencies for 1L MoS₂ on Au (Al₂O₃). (c) Behavior of the E_{2g} and A_{1g} peak frequencies as a function of the number of layers for MoS₂ on Au (filled squares and triangles) and for MoS₂ on Al₂O₃ (open squares and triangles). (d) Plot of the peaks frequency difference $\Delta\omega$ as a function of the number of layers for MoS₂ on Au (filled red circles) and MoS₂ on Al₂O₃ (empty red circles).

For both substrates, the A_{1g} peak frequencies (filled and empty triangles) exhibit a similar increasing trend with increasing the MoS₂ thickness. In particular, for thin MoS₂ membranes (1L-4L) the A_{1g} peak on MoS₂/Au (filled triangles) is slightly blue shifted with respect to MoS₂/Al₂O₃ (empty triangles), whereas the two frequencies converge to the same value for bulk samples. On the other hand, the E_{2g}

This is the author's peer reviewed, accepted manuscript. However, the online version of record will be different from this version once it has been copyedited and typeset.

PLEASE CITE THIS ARTICLE AS DOI: 10.1063/1.50062106

peak frequencies (filled and empty squares) show very different trends on the two substrates. While the decreasing E_{2g} peak frequency with increasing the MoS_2 thickness on Al_2O_3 (empty squares) is fully coherent with the reported literature results for MoS_2 on insulating substrates [20], this peak exhibits an anomalous behavior in the Au case (filled squares). In fact, for 1L MoS_2 on Au the E_{2g} is significantly red-shifted (by $\sim 2 \text{ cm}^{-1}$) with respect to 1L MoS_2 on Al_2O_3 . Its frequency increases from 1L to 2L MoS_2 on Au and remains almost constant for thicker membranes. Noteworthy, for bulk samples, the E_{2g} peak frequencies exhibit the same values on the two substrates. Figure 3(d) shows an increasing behavior of the peaks frequency difference $\Delta\omega$ as a function of the number of MoS_2 layers for the two different substrates. Furthermore, starting from a significantly larger value of $\Delta\omega \approx 21.2 \text{ cm}^{-1}$ for 1L MoS_2 on Au as compared to $\Delta\omega \approx 18.5 \text{ cm}^{-1}$ for 1L MoS_2 on Al_2O_3 , the difference between the measured $\Delta\omega$ values is gradually reduced with increasing the number of layers, reaching approximately the same value of $\sim 25 \text{ cm}^{-1}$ for bulk samples.

It is worth mentioning that the measured $\Delta\omega$ value in the Raman spectra of MoS_2 is generally taken as a straightforward way to estimate the number of layers. In particular, for 1L MoS_2 exfoliated/grown on common insulating substrates (such as SiO_2) the reported values of the separation $\Delta\omega$ between E_{2g} and A_{1g} vibrational peaks can range from $\sim 18 \text{ cm}^{-1}$ to $\sim 20 \text{ cm}^{-1}$ [20]. Hence, the value of 18.5 cm^{-1} for our 1L MoS_2 exfoliated on Au and transferred to the $\text{Al}_2\text{O}_3/\text{Si}$ substrate is in the range of the commonly reported literature values. In particular, it is very close to the value measured on 1L MoS_2 flakes directly exfoliated on Al_2O_3 [21]. On the other hand, for as-exfoliated 1L MoS_2 on Au an anomalously large value of $\Delta\omega = 21.2 \text{ cm}^{-1}$ is measured. Since the Au-assisted exfoliation is a very clean process (simply achieved by pressing the fresh surface of the bulk MoS_2 stamp onto the as-deposited Au film), the large $\Delta\omega$ value cannot be explained by the presence of impurities at MoS_2/Au interface or on MoS_2 surface. On the other hand, its origin is the strong interaction between MoS_2 and the Au substrate [19].

The interaction with the substrate, particularly relevant in the case of ultra-thin MoS₂ membranes, can result both in doping effects, associated to charge transfer phenomena, and in tensile or compressive strain effects. The E_{2g} and A_{1g} Raman modes are known to be related to the strain (ϵ) and doping (n) of MoS₂ membranes. In particular, a quantification of the strain type (tensile/compressive) and percentage, as well as of the doping type and carrier density induced on 1L MoS₂ by the gold and Al₂O₃ substrates have been carried out using the following equations:

$$\omega_{E_{2g}} = \omega_{E_{2g}}^0 - 2\gamma_{E_{2g}} \omega_{E_{2g}}^0 \epsilon + k_{E_{2g}} n \quad (1)$$

$$\omega_{A_{1g}} = \omega_{A_{1g}}^0 - 2\gamma_{A_{1g}} \omega_{A_{1g}}^0 \epsilon + k_{A_{1g}} n. \quad (2)$$

Here, $\gamma_{E_{2g}}=0.68$ and $\gamma_{A_{1g}}=0.21$ are the two Grüneisen parameters, correlating the strain ϵ and the E_{2g} and A_{1g} peaks positions for 1L MoS₂ [23], while $k_{E_{2g}}=-0.33\times 10^{-13}$ cm and $k_{A_{1g}}=-2.2\times 10^{-13}$ cm are the shift rates of the Raman peaks as a function of the electron density n (in cm⁻²) [22]. Furthermore, $\omega_{E_{2g}}^0=385$ cm⁻¹ and $\omega_{A_{1g}}^0=405$ cm⁻¹ are the literature values of the E_{2g} and A_{1g} peaks frequencies for a suspended 1L MoS₂ membrane under 532 nm excitation [23], which represents the best approximation of an ideally unstrained and undoped 1L MoS₂. According to Eqs. (1) and (2), a biaxial tensile strain $\epsilon\approx 0.21\%$ and a p-type doping $n\approx -0.25\times 10^{13}$ cm⁻² were estimated for 1L MoS₂ exfoliated on Au, which was converted into a biaxial compressive strain $\epsilon\approx -0.25\%$ and n-type doping $n\approx 0.5\times 10^{13}$ cm⁻² after transfer to the Al₂O₃ substrate. Such n-type behaviour is consistent with the unintentional doping type commonly reported for exfoliated or CVD-grown MoS₂, which has been associated to the presence of defects (e.g. sulphur vacancies) or other impurities in the MoS₂ lattice [24]. In the case of 1L MoS₂ on Au, a strong electron transfer to the substrate is guessed, which overcompensates the native n-type doping, resulting in a net p-type behaviour. Furthermore, the tensile strain for 1L MoS₂ on Au can be ascribed to the lattice mismatch between MoS₂ and the Au surface, mostly exposing (111) orientation [25,26].

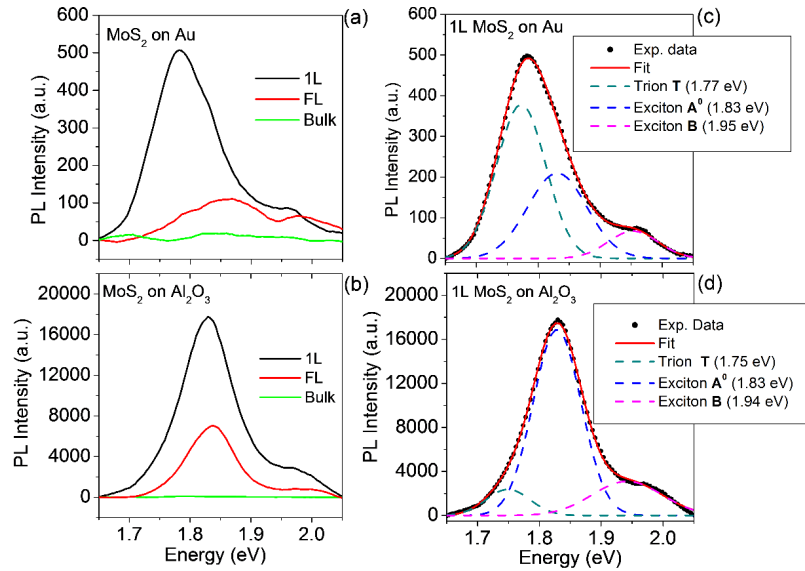


Figure 4. Photoluminescence spectra under 532 nm excitation for 1L, FL and bulk MoS₂ on Au (a) and Al₂O₃ substrate (b). Deconvolution of PL spectra for (c) 1L MoS₂ on Au and (d) 1L MoS₂ on Al₂O₃. Three different components were identified: the trion peak T, the exciton peak A⁰ and the exciton peak B.

Besides influencing the vibrational properties, the interaction with the substrate is expected to have an impact also on the optical emission behavior of MoS₂. Fig.4(a) and (b) illustrate the results of μ -PL analyses performed at room temperature under 532 nm excitation on MoS₂ areas with different thickness on the Au and Al₂O₃ substrates. In particular, the black, red and green lines represent the PL spectra for 1L, FL and bulk MoS₂. In order to perform a reliable comparison of the PL signal on the two different substrates, for each spectrum the intensities were normalized to the intensity of the MoS₂ Raman peaks. In this way, the comparison of the PL intensities between Fig.4(a) and (b) demonstrates a quenching (~ 4 times) of the emission yield for 1L MoS₂ exfoliated on Au as compared to 1L MoS₂ transferred onto Al₂O₃. A reduction of the relative PL intensities when increasing the MoS₂ thickness from 1L to FL was

This is the author's peer reviewed, accepted manuscript. However, the online version of record will be different from this version once it has been copyedited and typeset.

PLEASE CITE THIS ARTICLE AS DOI: 10.1063/1.50062106

This is the author's peer reviewed, accepted manuscript. However, the online version of record will be different from this version once it has been copyedited and typeset.

PLEASE CITE THIS ARTICLE AS DOI: 10.1063/1.50062106

consistently observed on both kinds of substrates, with the intensity approaching to zero in bulk samples according to the indirect bandgap. Looking more in details at PL emission for 1L MoS₂, for both substrates the PL spectra exhibit a main intense peak at lower energy and another weaker peak at higher energy, associated to the MoS₂ band splitting due to spin-orbit coupling [27,28]. While the main peak for 1L MoS₂ on Al₂O₃ is located at 1.84 eV, similarly to what typically reported on other insulating substrates [29], a significant red shift to 1.79 eV is observed for 1L MoS₂ on the Au substrate. To get a deeper insight in the PL emission mechanisms of 1L MoS₂ on the two different substrates, a deconvolution of the two representative spectra has been carried out, as reported in Fig.4(c) and (d). In both cases, the best fit was obtained considering three Gaussian peaks, which were associated to a trionic contribution T (green dashed line), and two excitonic contributions, i.e. the exciton A⁰ (blue) and the exciton B (grey) [30,31,32]. Differently from neutral excitons, consisting of a bound electron/hole pair, trions are charged quasiparticles formed by two electrons and a hole [30]. Noteworthy, while the exciton peak A⁰ at 1.84 eV represents the main PL contribution for 1L MoS₂ on Al₂O₃, the trion peak T at 1.78 eV appears to be the dominant one in the case of 1L MoS₂ on Au. Finally, the B exciton peak at 1.94 eV for 1L MoS₂ on Al₂O₃ exhibits a significantly higher full width at half maximum (FWHM) with respect to the corresponding peak (at 1.96 eV) for 1L MoS₂ on Au. As indicated in the labels of Fig.4(c) and (d), the T, A⁰ and B peaks obtained by the deconvolution are slightly blue-shifted in the case of 1L MoS₂ on Au with respect to 1L MoS₂ on Al₂O₃. However, the overall red shift of the PL spectra for 1L MoS₂ on Au is due to the higher intensity of the trion contribution. As reported in recent theoretical studies [33,34], this effect can be ascribed to the high polarizability of the metal substrate and to the low MoS₂/Au equilibrium distance enhancing the trion population and at the same time quenching the overall emission amplitude [6]. Noteworthy, in the case of FL MoS₂ on Au (Fig.4(a)) the main PL peak appears to be broader and blue-shifted with respect to the monolayer one, and its energy is closer to that of FL MoS₂

This is the author's peer reviewed, accepted manuscript. However, the online version of record will be different from this version once it has been copyedited and typeset.

PLEASE CITE THIS ARTICLE AS DOI: 10.1063/1.50062106

on Al₂O₃. This observation suggests that the increase of the MoS₂ thickness results in a reduced effect of the substrate not only on vibrational properties but also on PL emission.

In conclusion, we have deeply investigated the substrate effects on the Raman and PL emission properties of cm² – wide MoS₂ membranes exfoliated on Au and subsequently transferred on an insulating Al₂O₃/Si substrate. For as-exfoliated 1L MoS₂ on Au, Raman spectra showed an anomalous large value of $\Delta\omega \approx 21.2 \text{ cm}^{-1}$ (due to the tensile strain and p-type doping induced by the substrate) as compared to the typical one ($\sim 18.5 \text{ cm}^{-1}$) measured after the transfer of 1L MoS₂ on Al₂O₃ and complete removal of Au. Such substrate-related differences, were found to gradually decrease while increasing the number of MoS₂ layers. These results have also practical implications, indicating that Raman spectroscopy should be used in combination with other physical characterizations (e.g. AFM or transmission electron microscopy) to unambiguously evaluate the number of MoS₂ layers. Furthermore, PL spectra for 1L MoS₂ on Au exhibit a strong quenching and an overall red-shift of the main emission peak at 1.79 eV, compared to the 1.84 eV peak position for 1L MoS₂ on Al₂O₃. Such red shift was explained in terms of a higher trion/exciton intensity ratio, indicating how the relative population of quasiparticles generated under light excitation is significantly affected by the 1L MoS₂/Au interaction.

These results will be relevant in view of the widespread applications of large-area MoS₂ membranes produced by the gold-assisted exfoliation in electronics and optoelectronics.

S. Di Franco (CNR-IMM) is acknowledged for the expert technical assistance in samples preparation. This work has been supported, in part, by MUR in the framework of the FlagERA-JTC2019 project ETMOS. Part of this work has been carried out in the Italian Infrastructure *Beyond-Nano Upgrade*.

The data that support the findings of this study are available from the corresponding author upon reasonable request.

This is the author's peer reviewed, accepted manuscript. However, the online version of record will be different from this version once it has been copyedited and typeset.

PLEASE CITE THIS ARTICLE AS DOI: 10.1063/5.0062106

References

- [1] B. Radisavljevic, A. Radenovic, J. Brivio, V. Giacometti, A. Kis, *Nat. Nanotech.* **6**, 147-150 (2011).
- [2] O. Lopez-Sanchez, D. Lembke, M. Kayci, A. Radenovic, A. Kis, *Nat. Nanotech.* **8**, 497-501 (2013).
- [3] Z. Yin, H. Li, Ho. Li, L. Jiang, Y. Shi, Y. Sun, G. Lu, Q. Zhang, X. Chen, H. Zhang, *ACS Nano* **6**, 74-80 (2012).
- [4] F. Giannazzo, *Nat. Electron.* **2**, 54–55 (2019).
- [5] J. Sun, X. Li, W. Guo, M. Zhao, X. Fan, Y. Dong, C. Xu, J. Deng, Y. Fu, *Crystals* **7**, 198 (2017).
- [6] M. Velický, G.E. Donnelly, W.R. Hendren, S. McFarland, D. Scullion, W.J.I. DeBenedetti, G.C. Correa, Y. Han, A.J. Wain, M.A. Hines, D.A. Muller, K.S. Novoselov, H.D. Abruña, R.M. Bowman, E.J.G. Santos, F. Huang, *ACS Nano* **2**, 10463-10472 (2018).
- [7] S.B. Desai, S.R. Madhvapathy, M. Amani, D. Kiriya, M. Hettick, M. Tosun, Y. Zhou, M. Dubey, J.W. Ager III, D. Chrzan, A. Javey, *Advanced Materials* **28**, 4053-4058 (2016).
- [8] G.Z. Magda, J. Pető, G. Dobrik, C. Hwang, L.P. Biró, L. Tapasztó, *Scientific Reports* **5**, 14714 (2015).
- [9] M. Velický, A. Rodriguez, M. Bouša, A.V. Krayev, M. Vondráček, J. Honolka, M. Ahmadi, G.E. Donnelly, F. Huang, H.D. Abruña, K.S. Novoselov, O. Frank, *J. Phys. Chem. Lett.* **11**, 6112-6118 (2020).
- [10] H. Häkkinen, *Nat. Chem.* **4**, 443 (2012).
- [11] S. M. Hus, R. Ge, P.-A. Chen, L. Liang, G. E. Donnelly, W. Ko, F. Huang, M.-H. Chiang, A.-P. Li, D. Akinwande, *Nat. Nanotech.* **16**, 58–62 (2021).
- [12] Y. Huang, Y.-H. Pan, R. Yang, L.-H. Bao, L. Meng, H.-L. Luo, Y.-Q. Cai, G.-D. Liu, W.-J. Zhao, Z. Zhang, L.-M. Wu, Z.-L. Zhu, M. Huang, L.-W. Liu, L. Liu, P. Cheng, K.-H. Wu, S.-B. Tian, C.-Z. Gu, Y.-G. Shi, Y.-F. Guo, Z. G. Gang, J.-P. Hu, L. Zhao, G.-H. Yang, E. Sutter, P. Sutter, Y.-L. Wang, W. Ji, X.-J. Zhou, H.-J. Gao, *Nat. Commun.* **11**, 1-9 (2020).
- [13] F. Liu, W. Wu, Y. Bai, S. H. Chae, Q. Li, J. Wang, J. Hone, X.-Y. Zhu, *Science* **367**, 903–906 (2020).
- [14] Y. Chen, M. Sun, *Nanoscale* **13**, 5594 (2021).
- [15] J. Fan, J. Song, Y. Cheng, M. Sun, *Results in Physics* **24**, 104110 (2021).
- [16] F. Giannazzo, G. Greco, F. Roccaforte, S.S. Sonde *Crystals*, **8**, 70 (2018).
- [17] A. Gnisci, G. Faggio, L. Lancellotti, G. Messina, R. Carotenuto, E. Bobeico, P. Delli Veneri, A. Capasso, T. Dikonimos, N. Lisi, *Phys. Stat. Sol. A* 1800555,1-9 (2018).
- [18] F. Giannazzo, G. Greco, E. Schilirò, R. Lo Nigro, I. Deretzis, A. La Magna, F. Roccaforte, F. Iucolano, S. Ravesi, E. Frayssinet, et al., *ACS Appl. Electron. Mater.* **1**, 2342–2354 (2019).

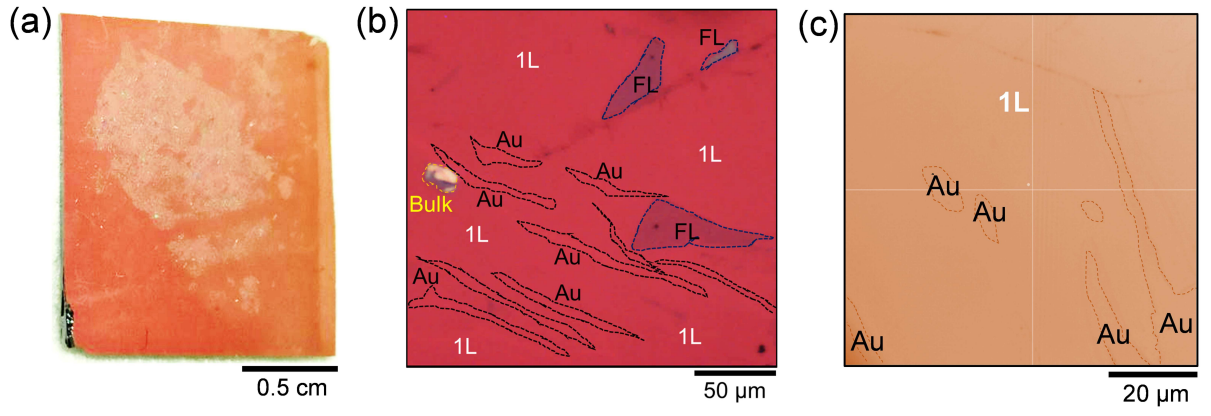
This is the author's peer reviewed, accepted manuscript. However, the online version of record will be different from this version once it has been copyedited and typeset.

PLEASE CITE THIS ARTICLE AS DOI: 10.1063/1.50062106

- [19] S. E. Panasci, E. Schilirò, G. Greco, M. Cannas, F. M. Gelardi, S. Agnello, F. Roccaforte, F. Giannazzo, *ACS Appl. Mater. Interfaces* **13**, 31248–31259 (2021).
- [20] C. Lee, H. Yan, L. E. Brus, T. F. Heinz, J. Hone, S. Ryu, *ACS Nano* **4**, 2695-2700 (2010).
- [21] J. Xu, L. Chen, Y.-W. Dai, Q. Cao, Q.-Q. Sun, S.-J. Ding, H. Zhu, D. W. Zhang, *Science Advances* **3**, e1602246 (2017).
- [22] B. Chakraborty, A. Bera, D.V.S. Muthu, S. Bhowmick, U. V. Waghmare, A. K. Sood, *Phys. Rev. B* **85**, 161403 (2012).
- [23] D. Lloyd, X. Liu, J. W. Christopher, L. Cantley, A. Wadehra, B. L. Kim, B.B. Goldberg, A.K. Swan, J. S. Bunch, *Nano Lett.* **16**, 5836-5841 (2016).
- [24] F. Giannazzo, G. Fisichella, A. Piazza, S. Agnello, F. Roccaforte, *Phys. Rev. B* **92**, 081307(R) (2015).
- [25] C. Gong, C. Huang, J. Miller, L. Cheng, Y. Hao, D. Cobden, J. Kim, R. S. Ruoff, R. M. Wallace, K. Cho, X. Xu, Y. J. Chabal, *ACS Nano* **7**, 11350–11357 (2013).
- [26] A. Bruix, J. A. Miwa, N. Hauptmann, D. Wegner, S. Ulstrup, S. S. Grønberg, C. E. Sanders, M. Dendzik, A. Grubisic Cabo, M. Bianchi, J. V. Lauritsen, A. A. Khajetoorians, B. Hammer, P. Hofmann, *Phys. Rev. B* **93**, 165422 (2016).
- [27] A. Molina-Sánchez, D. Sangalli, K. Hummer, A. Marini, L. Wirtz, *Phys. Rev. B* **88**, 045412 (2013).
- [28] K. F. Mak, C. Lee, J. Hone, J. Shan, T.F. Heinz, *Phys. Rev. Lett.* **105**, 136805 (2010).
- [29] A. Splendiani, L. Sun, Y. Zhang, T. Li, J. Kim, C.-Y. Chim, G. Galli, F. Wang, *Nano Lett.* **10**, 1271–1275 (2010).
- [30] K. F. Mak, K. He, C. Lee, G. H. Lee, J. Hone, T. F. Heinz, J. Shan, *Nature Materials* **12**, 207-211 (2013).
- [31] K. Kheng, R. T. Cox, M. Y. d'Aubigné, F. Bassani, K. Saminadayar, S. Tatarenko, *Phys. Rev. Lett.* **71**, 1752 (1993).
- [32] N. Scheuschner, O. Ochedowski, A. M. Kaulitz, R. Gillen, M. Schleberger, J. Maultzsch, *Phys. Rev. B* **89**, 125406 (2014).
- [33] M. Drüppel, T. Deilmann, P. Krüger, M. Rohlfing, *Nature Commun.* **8**, 1-7 (2017).
- [34] Y. V. Zhumagulov, A. Vagov, D. R. Gulevich, P. E. Faria Junior, V. Perebeinos, *J. Chem. Phys.* **153**, 044132 (2020).

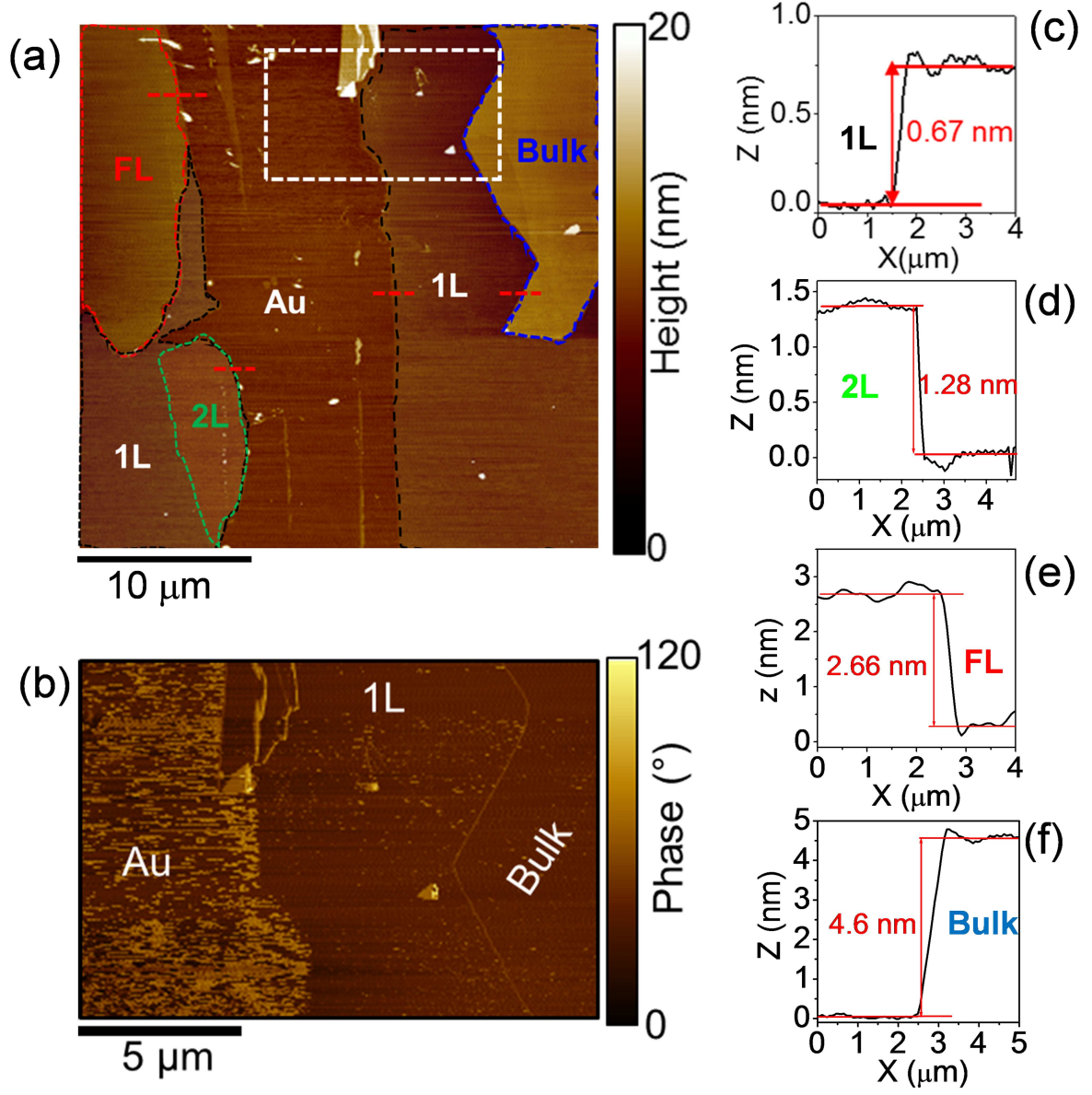
This is the author's peer reviewed, accepted manuscript. However, the online version of record will be different from this version once it has been copyedited and typeset.

PLEASE CITE THIS ARTICLE AS DOI: 10.1063/1.50062106



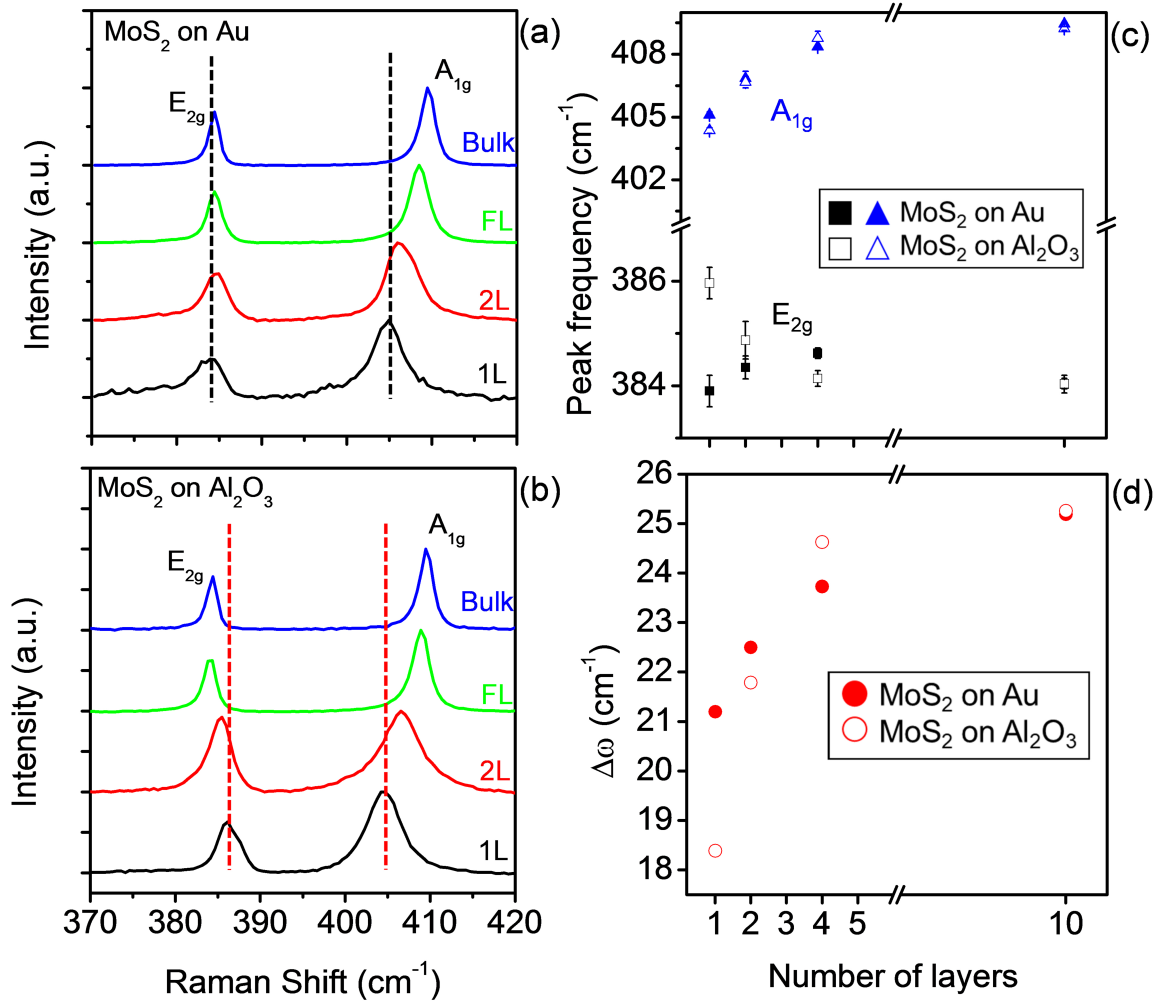
This is the author's peer reviewed, accepted manuscript. However, the online version of record will be different from this version once it has been copyedited and typeset.

PLEASE CITE THIS ARTICLE AS DOI: 10.1063/5.0062106



This is the author's peer reviewed, accepted manuscript. However, the online version of record will be different from this version once it has been copyedited and typeset.

PLEASE CITE THIS ARTICLE AS DOI: 10.1063/1.50062106



This is the author's peer reviewed, accepted manuscript. However, the online version of record will be different from this version once it has been copyedited and typeset.

PLEASE CITE THIS ARTICLE AS DOI: 10.1063/1.50062106

